Journal of Inflammation Research

Dovepress
open access to scientific and medical research

Open Access Full Text Article

ORIGINAL RESEARCH

The extracellular matrix of eggshell displays anti-inflammatory activities through NF-κB in LPS-triggered human immune cells

This article was published in the following Dove Press journal:
Journal of Inflammation Research
4 July 2017
Number of times this article has been viewed

Tram T Vuong[1]
Sissel B Rønning[1]
Henri-Pierre Suso[2]
Ralf Schmidt[2]
Kristian Prydz[3]
Marlene Lundström[3]
Anders Moen[3]
Mona E Pedersen[1]

[1]Department of Raw Materials and Process Optimisation, Nofima AS, Ås, [2]Biovotec AS, [3]Department of Biosciences, University of Oslo, Oslo, Norway

Abstract: Avian eggshell membrane (ESM) is a natural biomaterial that has been used as an alternative natural bandage on burned and cut skin injuries for >400 years in Asian countries, and is available in large quantities from egg industries. Our aim was to characterize ESM that was separated and processed from egg waste, and to study whether this material possesses anti-inflammatory properties, making it suitable as an ingredient in industrial production of low cost wound healing products. Our results show that the processed ESM particles retain a fibrous structure similar to that observed for the native membrane, and contain collagen, and carbohydrate components such as hyaluronic acid and sulfated glycosaminoglycans, as well as N-glycans, mostly with uncharged structures. Furthermore, both processed ESM powder and the ESM-derived carbohydrate fraction had immunomodulation properties in monocytes and macrophage-like cells. Under inflammatory conditions induced by lipopolysaccharide, the ESM powder and the isolated carbohydrate fraction reduced the activity of the transcription factor nuclear factor-κB. The expression of the immune regulating receptors toll-like receptor 4 and ICAM-1, as well as the cell surface glycoprotein CD44, all important during inflammation response, were down-regulated by these fractions. Interestingly, our experiments show that the two fractions regulated cytokine secretion differently: ESM depressed inflammation by increased secretion of the anti-inflammatory cytokine IL-10 while the carbohydrate fraction reduced secretions of the pro inflammatory cytokines IL-1β and IL-6. Also, the phosphorylation of p65 and p50 subunits of nuclear factor-κB, as well as nuclear localization, differed between processed ESM powder and carbohydrate fraction, suggesting different down-stream regulation during inflammation. In conclusion, processed ESM powder and its soluble carbohydrate components possess anti-inflammatory properties, demonstrating the potential of ESM as a novel biological wound dressing for treatment of chronic inflammatory wounds.

Keywords: eggshell membrane, anti-inflammation, cytokine secretions, signal transduction pathways, NF-κB, THP-1 cells, wound healing, carbohydrates, hyaluronic acid

Introduction

Skin wound healing is a stepwise and highly regulated process that consists of an initial inflammatory phase, a proliferative repair phase, and finally a remodeling phase, resulting in wound closure.[1] Deregulation of any of these steps results in impaired healing, such as chronic hard to heal ulcers or excessive scarring. Treatment of hard to heal ulcers is a huge economic burden to the society, and finding new and low cost therapeutic treatments would therefore be highly warranted. Eggshell membrane (ESM) is an interesting biological material in this perspective. It has been used as an alternative natural bandage on burned and cut skin injuries for >400 years in Asian

Correspondence: Tram Thu Vuong
Nofima AS, Postboks 210, NO-1431, Ås, Norway
Tel +47 6497 0134
Fax +47 6497 0333
Email tram.thu.vuong@nofima.no

submit your manuscript | www.dovepress.com
Dovepress
http://dx.doi.org/10.2147/JIR.S130974

countries. Recently, a study has demonstrated its positive effect in a rat wound model, by decreasing wound closure time.[2] So far, mechanisms of how ESM actually works on wound healing, or the bioactive components involved in this process, are far from understood.

ESM is a functional equivalent of extracellular matrix (ECM) during egg development, and functions as a scaffold for biomineralization to fabricate the eggshell. ESM is a bioactive material that consists of a structural network of complex carbohydrates such as the glycosaminoglycans (GAGs),[3] cysteine-rich eggshell membrane proteins (CREMPS), and collagens (type I, V, and X), together with other glycoproteins as ovotransferrin and Ca-regulatory proteins.[4–7] In addition to its role in biomineralization, ESM is essential for fabrication of the calcified shell as a defense against bacterial penetration, due to the content of antibacterial proteins.[8] Recently, different GAG structures with hyaluronic acid (HA) as the major part have been identified in raw ESM.[3] GAGs resident in the ESM are interesting candidates as mediators of wound healing, as they are known to play both pro-and anti-inflammatory roles.[9–11] Heparan sulfate (HS) interacts with cytokines/chemokines and generates cytokine gradients important for recruitment and infiltration of leukocytes into the wound site.[12] So far, ESM-derived GAGs or other carbohydrates of the ESM have not been studied in relation to inflammation. Collagens present in ESM are also interesting bioactive candidates, as collagen is today an ingredient in different wound healing products, and the structural properties of collagen fibers with effect on cell proliferation and remodeling activities have been outlined.[13] The functions of CREMPS, recently discovered in large quantities in ESM and shown to be avian specific,[14] has not been determined, but their presence in large amounts in the ESM indicates that these proteins also could be interesting candidates in relation to wound healing. Hen egg white glycoprotein, ovotransferrin, also present in ESM, has recently been demonstrated to possess anti-inflammatory properties.[15] Some studies have indicated anti-inflammatory properties of hydrolyzed and solubilized ESM.[16–19] It is unknown whether processed ESM powder possesses the same properties. N-glycans on glycoproteins have also been reported to have the capacity to influence inflammatory processes.[20,21] The dominating N-glycan structures consisted of six N-acetyl-hexosamines and three hexoses, while charged N-glycans were less prominent.

The first step in wound healing, the inflammatory phase, is crucial for the outcome of the wound healing process. Macrophages are involved in the first line of defense against pathogens; they are stimulated by the cytokine microenvironment generated by neutrophils and can become differently activated.[1] Not only do they play a role in sustaining the inflammatory response, but also in promoting its resolution. During infection, macrophage functions are critical for elimination of pathogens and secretion of growth factors, chemokines, and cytokines, activating the next phase of wound healing (proliferative phase). However, uncontrolled inflammatory responses can induce injury of the tissue environment and must be repressed to allow repair. In the presence of pathogens or bacterial components, such as lipopolysaccharide (LPS), macrophages secrete proinflammatory cytokines (such IL-1β, IL-6, IL-8, and tumor necrosis factor [TNF]-α). Then the cells start producing anti-inflammatory cytokines (like IL-4, IL-10, and IL-13) to resolve the pro inflammatory response (for review).[22] Different receptors present on the cell surface interact with inflammatory signals or ECM residents and trigger signaling pathways responsible for macrophage activation and specific cytokine production. The innate immune system relies on pathogen receptors, like toll-like receptor 4 (TLR4) in order to induce a systemic inflammation response upon bacterial invasion. This interaction induces a downstream signaling cascade of different signal transduction adaptor proteins, with the MyD88-pathway and nuclear factor-κB (NF-κB) transcription factor activation as one major pathway.[23,24] Endothelial adhesion molecules, including ICAM-1, are critical for T-cell activation and leukocyte recruitment to the inflammation site, and therefore play important roles during the immune response. Pro inflammatory cytokines, such as IL-1 and TNF-α, activate endothelial cells at the site of inflammation and lead to an up regulation of ICAM-1.[25] ICAM-1 also regulates the immune response in the monocyte/macrophage system in relation to microgravity,[26] and is upregulated in response to inflammatory triggers such as LPS.[27] The cell surface glycoprotein CD44 antigen functions as cell–cell and cell–ECM adhesion molecule, influencing cell migration, as well as endocytic processes and metabolism of macrophages.[28] CD44 is the predominant receptor for the high molecular mass HA that reduce pro inflammatory cytokine production in mice.[29]

Previous in vitro studies of solubilized ESM hydrolysates demonstrated their ability to influence cytokine expression in peripheral blood mononuclear cells.[16] In this study, we aim to reveal whether less processed ESM powder, mimicking intact ECM intended for industrial production of a low cost wound healing product, has anti-inflammatory properties. We also investigated whether the carbohydrate part of the ESM powder displays any immunomodulatory effects.

Materials and methods

Preparation of ESM powder

The raw material used for the studies is industrial ESM from Nortura (Oslo, Norway), which is derived from approved food quality hen eggs. The eggshell is processed and ESM produced and harvested by using a patented process owned by Biovotec (international application: WO 2015/058790 A1). The harvested ESM was then washed, purified, dried, and milled to small particle under 100 µ. After gamma irradiation at 25 kGy, the ESM powder was analyzed and examined by infrared spectroscopy before applying to cell cultures.

Scanning electron microscopy

ESM powder was mounted on an aluminum stub using double-sided tape coated with carbon. The sample was then coated with gold/palladium using a sputter coater (SC7640 Sputter Coater, Auto/Manual High Resolution, Quorum Technologies Ltd, East Sussex, UK) and examined by environmental scanning electron microscope (Zeiss EVO-50-EP, Cars Zeiss SMT Ltd., Cambridge, UK).

Picrosirius red staining and light microscope

ESM powder was stained with Picrosirius Red Stain assay kit (Polysciences Inc., Eppelheim, Germany) according to the protocol. Briefly, the samples were stained for 2 min in the staining solution before following further steps in the protocol, and rinsed with distilled water in the end before being sprinkled on poly-L-lysine-coated glass slides and examined by light microscope (Leica Microsystems, Nussloch GmbH, Nussloch, Germany).

Glycosaminoglycan analysis by high performance liquid chromatography (HPLC)

Extraction of 1 g of ESM powder was performed in 10 mL of 4% sodium dodecyl sulfate (SDS), 5.6 M urea, 0.1 M Tris-buffer, pH 7.6 with protease inhibitors by mixing overnight at 4°C. Diethylaminoethyl-Sephacel columns (1 mL) were prepared and washed with 10 mL of 50 mM phosphate buffer (pH 7.4), containing 0.15 M NaCl. The sample (1.5 mL) was applied to the column at a slow flow rate (1 drop/8–10 s). The column was washed with 15 mL of 50 mM phosphate buffer (pH 7.4) containing 0.15 M NaCl, and then with 10 mL of 50 mM phosphate buffer (pH 7.4) containing 0.3 M NaCl, and eluted with 10 mL of 50 mM phosphate buffer (pH 7.4) containing 1 M NaCl. Samples of ~100 mg were prepared for each HPLC run. Parallel samples were treated with either chondroitinase ABC (cABC) from Sigma Aldrich Co, (St Louis, MA, USA), which degrades both HA and chondroitin sulfate (CS) into disaccharides, or cABC from Amsbio (AMS Biotechnology Ltd, Abingdon, UK), which essentially only degrades CS during incubations for a shorter time. The samples were incubated with cABC for 15 min in 33 mM Tris-HCl, 33 mM sodium acetate, pH 8.0. In addition, the samples were also treated with heparitinases I, II, and III for breaking down HS.[30]

N-glycan analysis by mass spectrometry

ESM powder (10 mg) was dissolved in 100 µL loading buffer (BioRad, Hercules, CA, USA). Proteins were resolved by SDS polyacrylamide gel electrophoresis (SDS-PAGE), stained with Coomassie, and the region of gel containing the proteins of interest was excised and subjected to in-gel trypsin (Sigma-Aldrich Co., St Louis, MA, USA) digestion and the resulting proteolytic fragments were analyzed by liquid chromatography (LC) mass spectrometry (MS). Reversed phase (C18) LC was performed using the Dionex Ultimate 3000 UHPLC systems (Thermo Fisher Scientific, Waltham, MA, USA). Peptide solution (5 µL) was injected into the extraction column: Acclaim PepMap µ-Precolumn, 5 µm resin (Thermo Fisher Scientific), and peptides were eluted in the back-flush mode onto the analytical column: Acclaim PepMap100 C18, 3 µm resin (Thermo Fisher Scientific). The mobile phase consisted of acetonitrile and MS grade water, both containing 0.1% formic acid. Chromatographic separation was achieved using a binary gradient from 3% to 50% of acetonitrile in water for 60 min, with 0.3 µL/min flow rate. The LC system was coupled via a nano-electrospray ion source to a Q Exactive Hybrid Quadrupole-Orbitrap Mass Spectrometer (Thermo Fisher Scientific). Peptide samples were analyzed with a high energy collisional dissociation fragmentation method, with normalized collision energy at 15%, acquiring one Orbitrap survey scan in the mass range of m/z 300–2000, followed by MS/MS of the 10 most intense ions in the Orbitrap.[31]

MS data were analyzed with an in-house maintained gallus protein sequence database using SEQUEST™ and Proteome Discoverer™ (Thermo Fisher Scientific). The mass tolerances of a fragment ion and a parent ion were set as 0.5 Da and 10 ppm, respectively. Methionine oxidation and cysteine carbamido-methylation were selected as variable modifications. MS/MS spectra of peptides corresponding to glycosylated eggshell peptides were manually searched by Qual Browser (v2.0.7). To connect the glycan to the peptide sequence, a search with each peptide mass was done in the

program Peptide Mass Tool against the sample database within 10 ppm window. The program displays a list of all possible peptide sequences with the specific searched mass, m/z. To find the correct glycopeptide, tryptic peptides with N-glycan sites were searched for in the list.

Carbohydrate extraction from ESM

Total protein was extracted from ESM by magnetic stirring 8 g ESM powder in 100 mL Tris-HCl buffer containing 4% SDS and 5.6 M urea for 4 days at 4°C. The mixture was centrifuged at 10,000× g for 30 min; then the supernatant was transferred to a new tube and further centrifuged for 30 min at 4000× *g*. The clear supernatant was dialyzed against dH_2O using dialysis tubes (MwCO 12,000–14,000 Da; Sigma-Aldrich) for 3 days and then freeze-dried. To remove the protein cores, the lyophilized powder was incubated with 1 mg/mL papain (Sigma-Aldrich) in 0.05 M Tris-HCl pH 7.4 and 5 mM L-cystein (Sigma-Aldrich) at 37°C for 48 h, with 2× refreshing with papain during this period. The papain-degraded material was dialyzed (MwCO 6,000–8,000 Da; Sigma-Aldrich) against dH_2O and freeze-dried. This fraction is called carbohydrate fraction and consists of various carbohydrate types, including glycans and GAGs >6,000 Da. The carbohydrate fraction was gamma sterilized before utilizing in cell experiments.

Cell cultures

The U937–3xκB-LUC cells (kind gift from Prof Rune Blomhoff),[32] a human monocytic cell line that was stably transfected with a luciferase reporter containing 3× NF-κB binding sites, were maintained in RPMI-1640 medium supplemented with 10% fetal bovine serum (FBS), 2 mM L-glutamine, 50 U/mL penicillin, 50 mg/mL streptomycin, and 75 μg/mL hygromycin. The human monocytic leukemia cell line THP-1 (purchased commercially; TIB-202TM; ATCC) was grown in suspension in complete RPMI 1640 culture medium supplemented with 10% FBS, 100 U/mL penicillin, 100 μg/mL streptomycin, 2 mM L-glutamine, and 0.05 mM β-mercaptoethanol. All solutions were obtained from Invitrogen (Carlsbad, CA, USA). Both cell lines were routinely maintained at 37°C in a humidified atmosphere of 5% CO_2 and sub-cultivated 3 times per week. Because the properties of the cells can change dramatically after prolonged periods in culture, both the THP-1 and U937–3xκB-LUC cells were replaced by early frozen stock after 25 and 20 passages, respectively.

U937 and NF-κB activity assay

All experiments with U937 cells were performed in medium with 2% FBS. In order to measure NF-κB activity, cells were seeded into white 96-well plates with a density of 1×10^5 cells/mL, 100 μL/well and incubated with either only 1 μg/mL LPS (*Escherichia coli* 055:B5; Sigma-Aldrich), or in the presence of various concentrations of ESM powder or carbohydrate fraction for 6 h. The NF-κB activity was determined by measuring the luciferase activity after addition of Bright-Glo Reagent (Promega, Madison, WI, USA) in accordance to the manufacturer's instructions. Cell viability was determined with CellTiter-Glo Luminescent Cell Viability Assay (Promega), with a cutoff value of 10% nonviable cells. Luminescence was detected using Glomax96 Microplate Luminometer (Promega).

Macrophage differentiation and treatments

The mature macrophage-like state of THP-1 cells was induced by treating the cells (10^6 cells/mL) for 72 h with 100 ng/mL of phorbol 12-myristate 13-acetate (PMA; Sigma-Aldrich) in 12-well culture plates. Differentiated, plastic-adherent cells were washed twice with sterile Dulbecco's phosphate-buffered saline (Sigma-Aldrich) and then incubated with fresh medium without PMA. Experiments were performed on day 2 after PMA removal. For all experiments, differentiated cells were treated with LPS (0.5 ng/mL) alone, or with LPS plus 1 mg/mL ESM or 0.125 mg/mL carbohydrate fraction for 20 h. The media were collected, centrifuged to remove cell debris, and then subjected to enzyme-linked immunosorbent assay (ELISA) for determination of cytokines secretions. The cells were washed twice with PBS and lysed in 350 μL RTL-buffer for subsequent RNA purification. In experiments studying signaling pathways, the cells were lysed in radioimmunoprecipitation assay buffer (RIPA) buffer before subjecting to Western blotting analysis.

ELISA

Levels of IL-1β, IL-6, and IL-10 in cell culture supernatants were determined using an ELISA. MaxiSorp ELISA plates (Nunc, Roskilde, Denmark) were pre-coated with mouse anti-human IL-1β (R&D Systems, Minneapolis, MN, USA), rat anti-human IL-6 or IL-10 antibodies (BD Biosciences, San Jose, CA, USA) suspended in coating buffer (0.1 M carbonate/bicarbonate buffer pH 9.6) overnight at 4°C. Unspecific binding sites were blocked by incubating with 5% bovine serum albumin in PBS for 1 h at room temperature. Samples and human recombinant IL-1β, IL-10 (R&D Systems), or IL-6 (BD Biosciences) standards diluted in high-performance ELISA (HPE) buffer (Sanquin, Amsterdam, Netherlands) were added and the plates were incubated for 1.5 h at

RT, before the biotinylated goat anti-human IL-1β (R&D Systems), rat anti-human IL-6 or IL-10 (BD Biosciences) antibodies were added and further incubated for 1 h. Next, streptavidin-horseradish peroxidase conjugate (BD Biosciences) in HPE buffer was added and incubated at RT for 30 min. Between each of these steps, the plates were washed at least 3 times with PBS containing 0.01% Tween-20. After the last washing step, TMB single solution (Thermo Fisher Scientific) was added and incubated for 10 min in dark at RT. The reaction was stopped by adding of 1 N H_2SO_4, and absorbance was measured at 450 nm using Titertek Multiscan plus MK II plate reader (Labsystems, Helsinki, Finland).

Quantitative real-time PCR

Total RNA from THP-1 macrophages after various treatments as indicated in Figure legends were isolated and purified using RNeasy mini kit (Qiagen, Hilden, Germany) and with DNAse step (Invitrogen) according to the manufacturer's instructions. A total of 200 ng of RNA was subjected to reverse transcriptase (RT)-reaction by Taqman Gold RT-PCR kit (Applied Biosystems, Foster City, CA, USA). The samples were diluted 4× before the application of 10 ng samples (in triplicates) to real-time PCR analysis in an ABI prism 7900HT Sequence detection system (Applied Biosystems), using TaqMan Gene expression assay (Applied Biosystems). Amplification of cDNA by 40 two-step cycles (15 s at 95°C for denaturation of DNA, 1 min at 60°C for primer annealing and extension) was performed, and cycle threshold (Ct) values were obtained graphically (Applied Biosystems, Sequence Detection System, Software version 2.2). Gene expression was normalized to the average value of elongation factor 1 alpha and ribosomal protein L32 (RPL32) and ΔCt values were calculated. Comparison of gene expression between samples (control and ESM treated) was derived from subtraction of ΔCt values between the two samples to give a ΔΔCt value, and relative gene expression (fold change) was calculated as $2^{-\Delta\Delta Ct}$ normalized to control. Applied Biosystems primer/probe assays were used in this study: CD44 (Hs01075861_m1), TLR4 (Hs01060206_m1), ICAM1 (Hs00164932_m1), EF1A1 (Hs00265885_g1), RPL32 (Hs00851655_g1).

Western blotting

After treatment with ESM powder or carbohydrate fraction, the cells were lysed in RIPA buffer (150 mM NaCl, 1% NP40, 0.5% Na-deoxycholate, 0.1% SDS in 50 mM Tris-HCl, pH 8) with the addition of phosphatase cocktail and protease inhibitor AEBSF (Sigma). The cell lysates of THP-1 macrophages were homogenized by centrifuging through QIA shredder mini spin columns (Qiagen). Equal volumes of cell lysates were subjected to SDS-PAGE on 12% Bis-Tris gel and blotted onto a cellulose membrane using iBlot dry blotting system (Invitrogen). The membranes were blocked in TBS-Tween with 2% ECL primer blocking agent (GE Healthcare, Chicago, IL, USA) for 1 h, incubated with primary antibodies: rabbit anti-HO-1, anti-TLR4 (LifeSpan Biosciences Inc., Seattle, WA, USA), anti-CD44 (Abcam, Cambridge, UK), anti-ICAM1, anti-phosho-p50 (Ser337, sc-101744), or anti-phospho-p65 (Ser311, sc-33039) (Santa Cruz Biotechnology, Santa Cruz Biotecnology Inc., Dallas, TX, USA) antibodies diluted in TBS-Tween with 1% ECL primer blocking agent overnight at 4°C. The membranes were washed 3× 5 min with TBS-Tween, incubated with secondary antibody ECL Plex goat-α-rabbit IgG-Cy5 (1:2500; GE Healthcare) for 1 h, and then washed 3×5 min in TBS-Tween. For loading control, the membranes were re-blotted with mouse antibody against α-tubulin (1:10.000; Sigma-Aldrich) and then with ECL Plex goat-α-mouse IgG-Cy3 antibody (1:2500; GE Healthcare). The membranes were air-dried before the protein bands were visualized and detected by Etan DIGE Imager (GE Healthcare) using Cy5 and Cy3 channel, respectively.

Fluorescent immunohistochemistry

Differentiated THP-1 cells, seeded out on Nunc 8 well chamber slides (Thermo Fisher Scientific) were fixed in 4% PFA (Reidel-de Haën, Seelze, Germany) for 15 min, washed 3 times in PBS before permeabilizing with 0.5% TritonX-100 in PBS for 15 min. After washing in PBS-tween, the cells were blocked using 5% milk in PBS-tween for 1 h before incubation with primary antibody for another 1 h. Subsequent incubation with secondary antibody was performed for 30 min before mounting using Dako fluorescent mounting medium (Dako Denmark A/S, Glostrup, Denmark). The cells were examined by fluorescence microscopy analysis (Zeiss Axio Obeserver Z1 microscope), and images were processed using Adobe Photoshop CS3. Primary antibodies used were rabbit phospho-p65 (Ser 311, sc-33039) and phospho-p50 (Ser 337, sc-101744), both from Santa Cruz Biotechnology. Secondary antibody used was Alexa 546-conjugated goat anti-rabbit (Life Technologies). Hoechst from Molecular probes (Invitrogen) was used to counterstain the nuclei.

Statistical analysis

Results are expressed as mean ± standard error mean (SEM) of at least three experiments with duplicate or triplicate determinations. Significant variance by treatments in

comparison to the untreated sample was determined by paired *t*-test performed in GraphPad Prism version 6.0 (GraphPad Software, La Jolla, CA, USA). Differences were considered significant at $p \leq 0.05$.

Results

The processed ESM powder has a fibrous structure and contained carbohydrates with HA as major GAG in addition to uncharged complex glycan structures

The ESM used in this study was milled into particles of <100 µ in size (see Materials and methods), and the structural properties after processing were characterized by scanning electron microscopy and staining with Picrosirius red, using light microscopy. A fibrous-like structure of the ESM powder containing collagens was clearly observed (Figure 1A, 1Bi). Examination of Picrosirius red-stained ESM powder using polarized light clearly outlined a yellow rim around the fiber structures, reflecting more heavily cross-linked collagens and thicker fibers (Figure 1Bii). ESM powder was also subjected to analysis by HPLC for determination of GAG types and their sulfation pattern. Table 1 shows that the main GAG type was HA, with 81% of total GAGs. The remaining GAGs were CS. Only negligible amounts of HS derived disaccharides (≤5% in sum) were detected in this sample.

The overall N-glycan structure was analyzed for a number of glycopeptides generated from various ESM proteins by proteolytic cleavage (Table 2). The dominating glycan structure is an uncharged N-glycan consisting of six N-acetylhexosamines and three hexoses. The distribution of different N-glycan structures for a particular glycan site is shown for the peptide QLEELLNR of the glycoprotein Clusterin (Figure 2). A bisecting N-acetyl-glucosamine (GlcNAc) is attached to the central mannose in all of the structures, which have antennae that terminate in GlcNAc, galactose, or N-acetyl-galactosamine. Similar structures were also observed for glycopeptides generated from ovalbumin-related protein (not shown).

Processed ESM powder possesses anti-inflammatory properties

In order to evaluate the anti-inflammatory property of our ESM product, different concentrations of ESM powder dissolved in cell culture medium were added to LPS-induced inflammatory U937–3xκB-LUC cells and the luciferase activity was measured after 6 h. Our result shows that ESM powder significantly reduced NF-κB activity in a dose-dependent manner (Figure 3A). The cell viability was not affected as assessed by Cell-Titer Glo assay kit (Figure 3B), demonstrating that the anti-inflammatory effect of ESM was not due to a reduced cell activity. Further, our results show that the ESM powder down-regulated the relative mRNA expression of cell surface receptors important during inflammation. After 20 h incubation with ESM powder in LPS-stimulated THP-1 macrophages, the relative mRNA expression of TLR4 and ICAM1 were significantly down-regulated compared to untreated cells, while the relative gene expression was unchanged for CD44 (Figure 4A). A similar effect of ESM was obtained for TLR4 and CD44 at

Table 1 The composition of glycosaminoglycan types in ESM

GAG type	Sulfation (S)	% record
HA	None S	81
CS	0-S	6
	4-S	12
	6-S	1
CS/DS	4-S,6-S	ND
HS	2-S	Negligible
	2-S,4-S	Negligible
	2-S,6-S	Negligible
	2-S,4-S,6-S	Negligible

Note: The number before -S indicates the sulfating position.
Abbreviations: ESM, eggshell membrane; GAG, glycosaminoglycan; HA, hyaluronic acid; CS, chondroitin sulfate; HS, heparan sulfate; DS, dermatan sulfate; ND, non-detected.

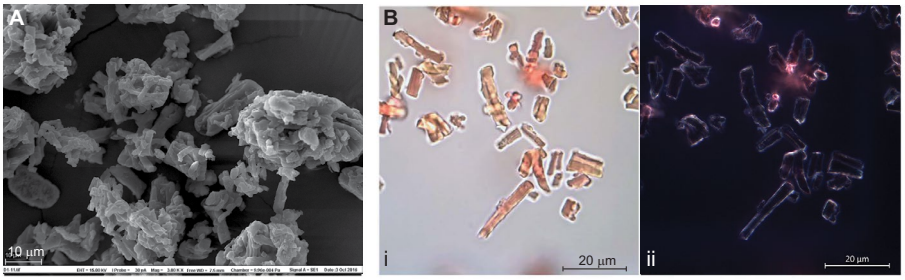

Figure 1 Structural characterization of the processed ESM powder.
Notes: Scanning electron micrograph of ESM showing fibrillary fibers (**A**). Collagen contained in ESM powder is determined by Picrosirius red staining and examined with light microscope (**Bi**) and by using polarized light (**Bii**).
Abbreviation: ESM, eggshell membrane.

Table 2 N-glycan structures identified in various ESM proteins

Protein	Modified peptide	Dominant glycan
Uncharacterized protein E1C037	FVPVDGCTCVNGTYMDESGK	6 N-acetyl hexosamines-3 hexoses
Uncharacterized protein E1BTF4	YNLTSILMALGMoxTDLFSR	6 N-acetyl hexosamines-3 hexoses
Uncharacterized protein F1NIT0	NNLSR	6 N-acetyl hexosamines-3 hexoses -1deoxyhexose
Mucin 6	YNMTLIWNKHMNFFIK	7 N-acetyl hexosamines-3 hexoses
Clusterin	QLEELLNR	6 N-acetyl hexosamines-3 hexoses
Clusterin	RYDDLLSAFQAEMLNTSSLLDQLNR	6 N-acetyl hexosamines-3 hexoses
Clusterin	LGNLTQGTDGFLQVTTVFSK	6 N-acetyl hexosamines-3 hexoses
Alpha-1-acid-glycoprotein	YATFTLFPGSHEDEFNVTEIMR	6 N-acetyl hexosamines-3 hexoses
Alpha-1-acid-glycoprotein	HNSTLTHEDGQVVSMoxAELIHSDKDLFILK	6 N-acetyl hexosamines-3 hexoses
Ovotransferrin	TAGWVIPMGLIHNR	6 N-acetyl hexosamines-3 hexoses
Ovoglobulin	AGAFNMTIPSMLTTATLAQK	6 N-acetyl hexosamines-3 hexoses
Apolipoprotein B	MNFSQELSGNTK	4 N-acetyl hexosamines-5 hexoses -1N-acetylneuraminic acid
Ovalbumin-related protein Y	ELLSEITRPNATYSLEIADK	5 N-acetyl hexosamines-3 hexoses

Abbreviation: ESM, eggshell membrane.

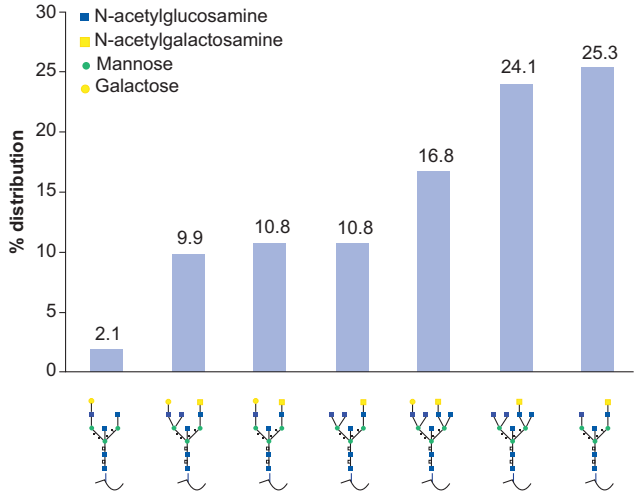

Figure 2 The distribution of N-glycan structures for a particular glycan site (QLEELLNR) of the glycoprotein Clusterin as determined by mass spectrometry.

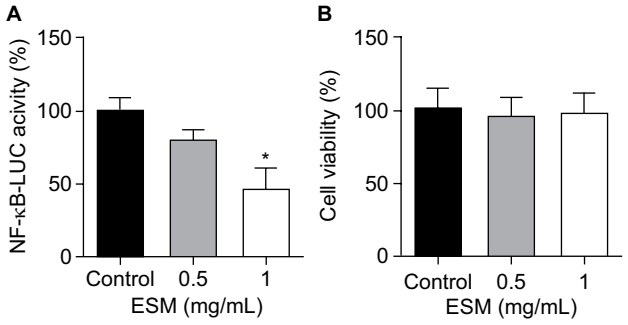

Figure 3 The effect of ESM powder on NF-κB activity and cell viability in LPS-induced inflammatory monocytes.

Notes: U937-3xκB-LUC cells were incubated with either 1 μg/ml LPS alone (control) or in combination with 0.5 or 1 mg/mL of ESM in cell culture medium for 6 h. Luciferase activity and cell viability were measured (luminescence). The NF-κB coupled inflammatory response was evaluated by measuring the luciferase activity in these cells (**A**). Cell viability was measured using Cell-Titer Glo cell viability assay (**B**). Each bar represents the mean ± SEM of at least three experiments performed in triplicates. (*p<0.05 by paired t-test).

Abbreviations: ESM, eggshell membrane; LPS, lipopolysaccharide; NF-κB, nuclear factor kappa B; SEM, standard error mean.

the protein level (Figure 4B). The protein level of ICAM1, however, was obviously unaffected by ESM, suggesting a differential regulation of this receptor at translational and post-translational level.

The anti-inflammatory activities of ESM powder was further investigated by examining the cytokine secretions. After 20 h incubating with ESM in LPS-stimulated THP-1 macrophages, we demonstrate that there was a moderate increased secretion of pro inflammatory IL-1β and IL-6 during the inflammatory response (Figure 5A, B). However, ESM treatment increased the secretion of the anti-inflammatory IL-10 by ~8.5 folds (Figure 5C), suggesting a dominating anti-inflammatory property of the processed ESM.

Further, we wanted to investigate whether the induced IL-10 production was in association with the M2 phase shift of macrophages. We then determined the expression of heme-detoxification enzyme heme oxygenase-1 (HO-1), which is a highly expressed protein in the anti-inflammatory M2 macrophages. The HO-1 protein level was increased after 20 h with ESM treatment. This increase was observed already after just 6 h of stimulation (Figure 6A). In accordance with this, IL-10 expression also increased after 6 h of ESM stimulation, although not significantly (Figure 6B).

Carbohydrate fraction of ESM powder possesses immunomodulation effects

To evaluate whether carbohydrates present in the ESM possess immunomodulatory effects similar to ESM powder, we extracted total carbohydrates in ESM (described under Materials and methods). The carbohydrate fraction contained sulfated and unsulfated GAGs, comparable to the GAGs identified in Table 1, as well as other types of glycans with

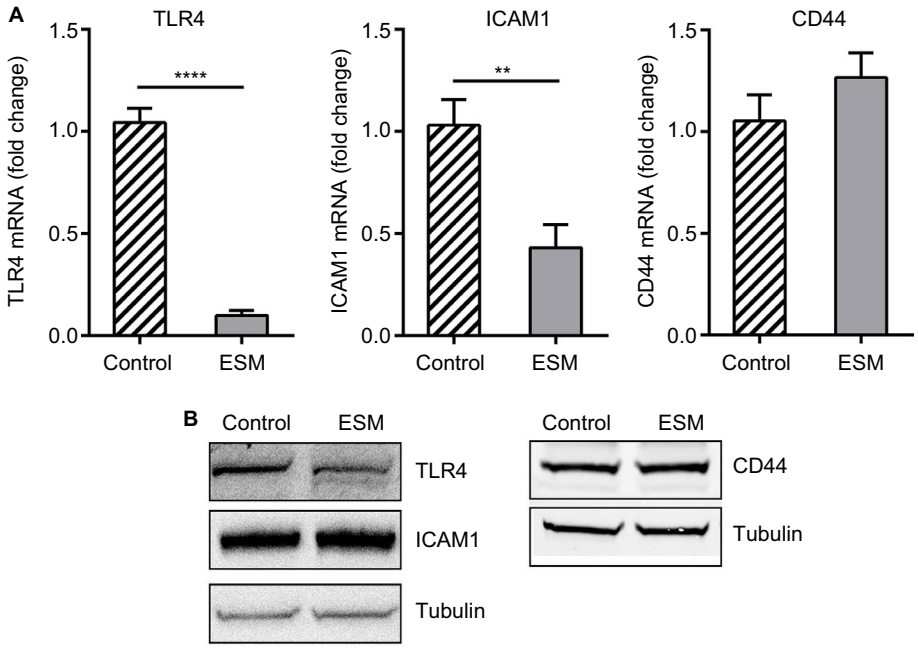

Figure 4 The effect of ESM powder on immune receptors.

Notes: PMA-differentiated THP-1 cells were incubated with 0.5 ng/ml LPS alone (control) or in combination with 1 mg/ml ESM for 20 h at 37°C. Cells were harvested and subjected to: (**A**) RT-PCR analysis for determining the mRNA expressions of TLR4, ICAM1 and CD44. The results are presented as mean ± SEM fold change relative to the control samples (n=3). (**p<0.01 and ****p<0.0001 by paired t-test), (**B**) Western blotting analysis for assessment of protein levels of TLR4, ICAM1 and CD44. A representative blot out of three independent experiment is presented. Tubulin was used as a loading control.

Abbreviations: ESM, eggshell membrane; LPS, lipopolysaccharide; PMA, phorbol 12-myristate 13-acetate; TLR4, toll-like receptor 4; ICAM1, intercellular adhesion protein 1; SEM, standard error mean.

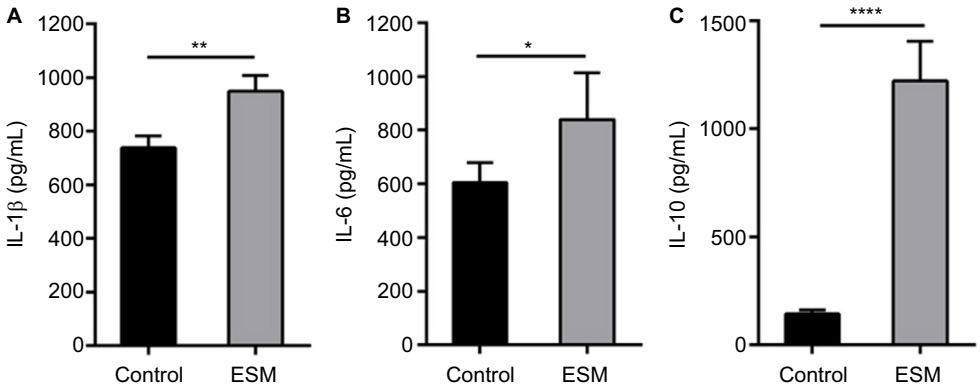

Figure 5 ESM powder up-regulates the pro- and anti-inflammatory cytokines secretions.

Notes: PMA-differentiated THP-1 cells were incubated with 0.5 ng/ml LPS alone (control) or in combination with 1 mg/ml ESM for 20 h at 37°C. Cell media were collected and the level of secreted pro inflammatory cytokines IL-1β (A) and IL-6 (B), and the anti-inflammatory cytokine IL-10 (C) were determined by ELISA. The results are presented as mean ± SEM protein level (n=5). (*p<0.05, **p<0.01 or ****p<0.0001 indicate a statistically significant change between control and ESM treated cells, determined by paired t-test).

Abbreviations: ELISA, enzyme-linked immunosorbent assay; ESM, eggshell membrane; LPS, lipopolysaccharide; PMA, phorbol 12-myristate 13-acetate; IL-1β, interleukin 1 beta; SEM, standard error mean.

molecular weight >6,000 Da. Anti-inflammatory properties of the carbohydrate fraction was similarly tested for the ESM powder. In line with the results from ESM powder (Figure 3), NF-κB activity declined with increasing carbohydrate concentrations. The NF-κB activity was almost completely inhibited at concentration 0.5 mg/mL (Figure 7A). However, the cell viability was also decreased by 70% by this concentration (Figure 7B), indicating a toxic effect of carbohydrate fraction at high concentration. Due to this reason, a concentration of 0.125 mg/mL carbohydrate fraction was used for subsequent cell experiments in this study.

A significant reduction in relative gene expression of TLR4 and ICAM1 was obtained with carbohydrate fraction (Figure 8A), similar to the effect obtained with ESM powder (Figure 4A). However, the CD44 gene expression tended to be down-regulated with carbohydrate fraction. As shown for the ESM powder, the TLR4 protein level was reduced while the level of ICAM1 and CD44 remained unchanged upon treat-

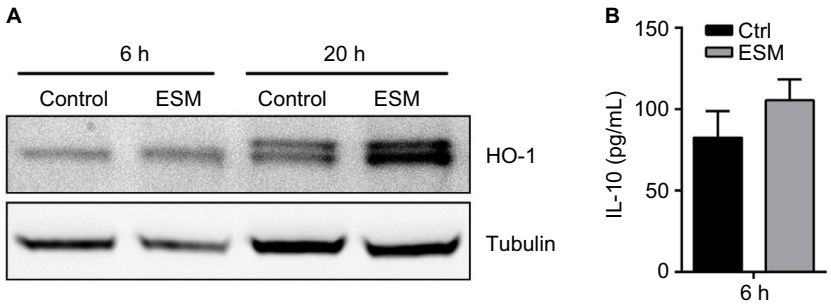

Figure 6 ESM powder increases the expression of HO-1 involved in inducement of macrophage M2 phenotype.
Notes: PMA-differentiated THP-1 cells were incubated with 0.5 ng/ml LPS alone (control) or in combination with 1 mg/ml ESM for 6 h and 20 h at 37°C. The cell media were collected and the cells were washed and lysed in RIPA buffer. (**A**) The protein level of HO-1 in cell lysates were determined by Western blotting and tubulin was used as loading control. A representative blot out of four independent experiments is shown. (**B**) The level of secreted anti-inflammatory cytokine IL-10 into the media after 6 h treatment were determined by ELISA. The results are presented as mean ± SEM protein level (n=3).
Abbreviations: Ctrl, control; ESM, eggshell membrane; ELISA, enzyme-linked immunosorbent assay; LPS, lipopolysaccharide; PMA, phorbol 12-myristate 13-acetate; HO-1, heme oxygenase 1; RIPA, radioimmunoprecipitation assay buffer; SEM, standard error mean.

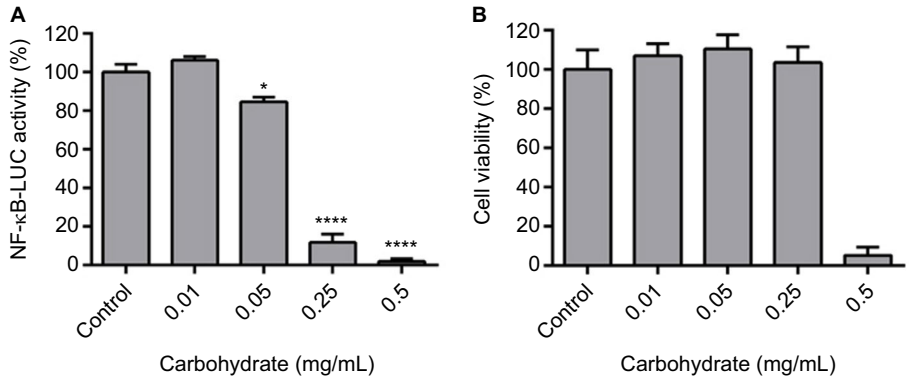

Figure 7 Effect of ESM derived carbohydrate fraction on NF-κB activity and cell viability in LPS-induced inflammatory monocytes.
Notes: U937-3xκB-LUC cells were incubated with either 1 μg/mL LPS alone (control) or in combination with various concentrations of carbohydrate fraction in cell culture medium for 6 h. Luciferase activity and cell viability were measured (luminescence). (**A**) The NF-κB coupled inflammatory response was evaluated by measuring the luciferase activity in these cells. (**B**) Cell viability was measured using Cell-Titer Glo cell viability assay. Each bar represents the mean ± SEM of three experiments performed in triplicates. *$p<0.05$ and ****$p<0.0001$ indicate a statistically significant change determined by paired t-test.
Abbreviations: ESM, eggshell membrane; LPS, lipopolysaccharide; NF-κB, nuclear factor kappa B; SEM, standard error mean.

ment with carbohydrate fraction (Figure 8B). Interestingly, our experiments demonstrated that the carbohydrate fraction influenced the cytokine secretion differently compared with treatment with ESM powder. While there was no effect on IL-10, carbohydrate fraction strongly reduced the secretion of pro inflammatory IL-1β and IL-6 (Figure 9).

ESM powder and carbohydrate fraction regulate down-stream TLR4 signaling pathways differently

To assess the activation of intracellular signaling pathways, the phosphorylation of p65 and p50 subunits of the nuclear factor NF-κB in LPS-induced inflammatory THP-1 cells were evaluated by Western blots. Interestingly, we showed that ESM and carbohydrate fraction differently regulated the activation of p65. While the ESM powder increased phosphorylation of p65, the carbohydrate fraction tended to reduce this phosphorylation (Figure 10A, upper panels). In contrast, neither of the two fractions had an effect on the phosphorylation level of the p50 units (Figure 10A, lower panels). Immunostaining of these cells, however, revealed a larger amount of phospho-p50 units, which relocated to the nuclei upon treatment with ESM powder. This translocation was not as evident for cells treated with the carbohydrate fraction (Figure 10B, right panels). The nuclear localization of phospho-p65 was unaffected by these treatments (Figure 10B, left panels).

Discussion

ESM is a well-known natural biomaterial that consists of collagens, glycoproteins, CREMPS, antibacterial proteins, and carbohydrates.[3] In its native form, ESM is characterized by a highly cross-linked fibrillary structure network.[33] It has been traditionally used as an alternative natural bandage on burned and cut skin injuries for >400 years in Asian countries. Here

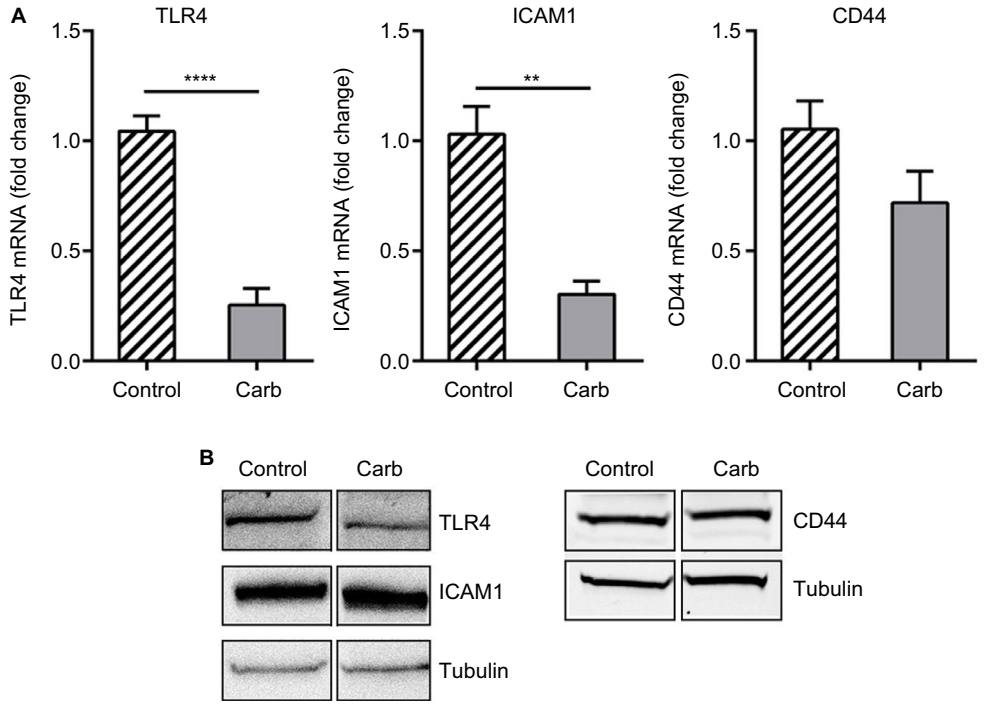

Figure 8 The effect of ESM derived carbohydrate fraction on immune receptors.
Notes: PMA-differentiated THP-1 cells were incubated with 0.5 ng/mL LPS alone (control) or in combination with 0.125 mg/mL carbohydrate fraction for 20 h at 37°C. Cells were harvested and total RNA was isolated before subjected to RT-PCR for determining the mRNA expressions of TLR4, ICAM1 and CD44 (**A**). The results are presented as mean ± SEM fold change relative to the control samples (n=3). $^{**}p<0.01$ and $^{****}p<0.0001$ indicate a statistically significant change determined by paired t-test. (**B**) Whole cell lysates were analyzed by Western blotting for assessment of TLR4, ICAM1 and CD44 protein levels. A representative blot out of four independent experiments is presented. Tubulin was used as a loading control.
Abbreviations: Carb, carbohydrate; PMA, phorbol 12-myristate 13-acetate; ESM, eggshell membrane; LPS, lipopolysaccharide; TLR4, toll-like receptor 4; SEM, standard error mean.

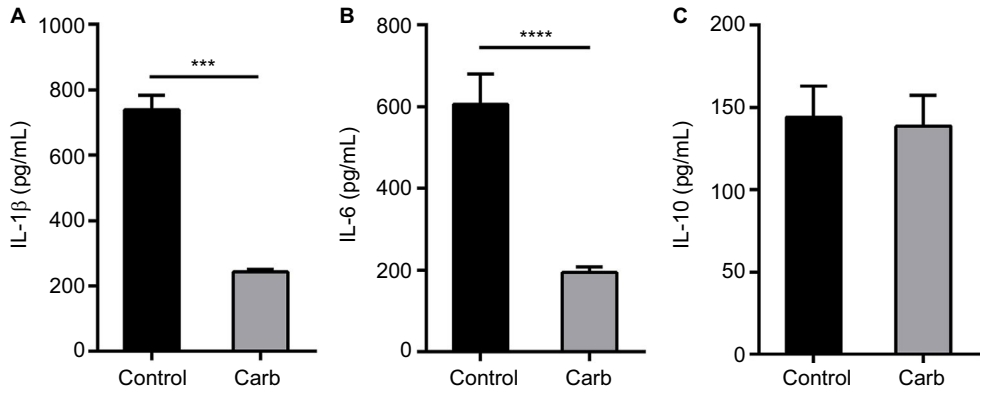

Figure 9 ESM-derived carbohydrate fraction depressed the secretion of proinflammatory cytokines IL-1β and IL-6.
Notes: PMA-differentiated THP-1 cells were incubated with 0.5 ng/mL LPS alone (control) or in combination with 0.125 mg/mL carbohydrate fraction for 20 h at 37°C. Cell media were collected and subjected to ELISA for measuring the level of secreted pro inflammatory cytokines IL-1β (**A**) and IL-6 (**B**), and the anti-inflammatory cytokine IL-10 (**C**). The results are presented as mean ± SEM protein level (n=5). ($^{***}p<0.001$ and $^{****}p<0.0001$ indicate a statistically significant change determined by paired t-test).
Abbreviations: ELISA, enzyme-linked immunosorbent assay; PMA, phorbol 12-myristate 13-acetate; ESM, eggshell membrane; LPS, lipopolysaccharide; IL-1β, interleukin 1 beta; SEM, standard error mean.

we demonstrate for the first time that powdered ESM material intended for industrial use, both retained the fiber-like structural properties and contained carbohydrate components mimicking the intact ESM. This ESM powder possessed anti-inflammatory properties, which suggests it to be a promising ingredient for formulation of wound healing products. Adding powdered ESM to LPS-induced immune cells strongly reduced NF-κB activity and induced the secretion of the anti-inflammatory key regulator IL-10. IL-10 is a potent anti-inflammatory cytokine that plays a crucial role in preventing inflammatory and autoimmune pathologies.[34] Further, ESM powder significantly down-regulated TLR4 and ICAM1 gene expression, both receptors important during inflammation responses. The role of TLRs in innate immune response is crucial, as the expression levels of these receptors reflect the sensitivity of immune cells to infections.[35–37] LPS binding to

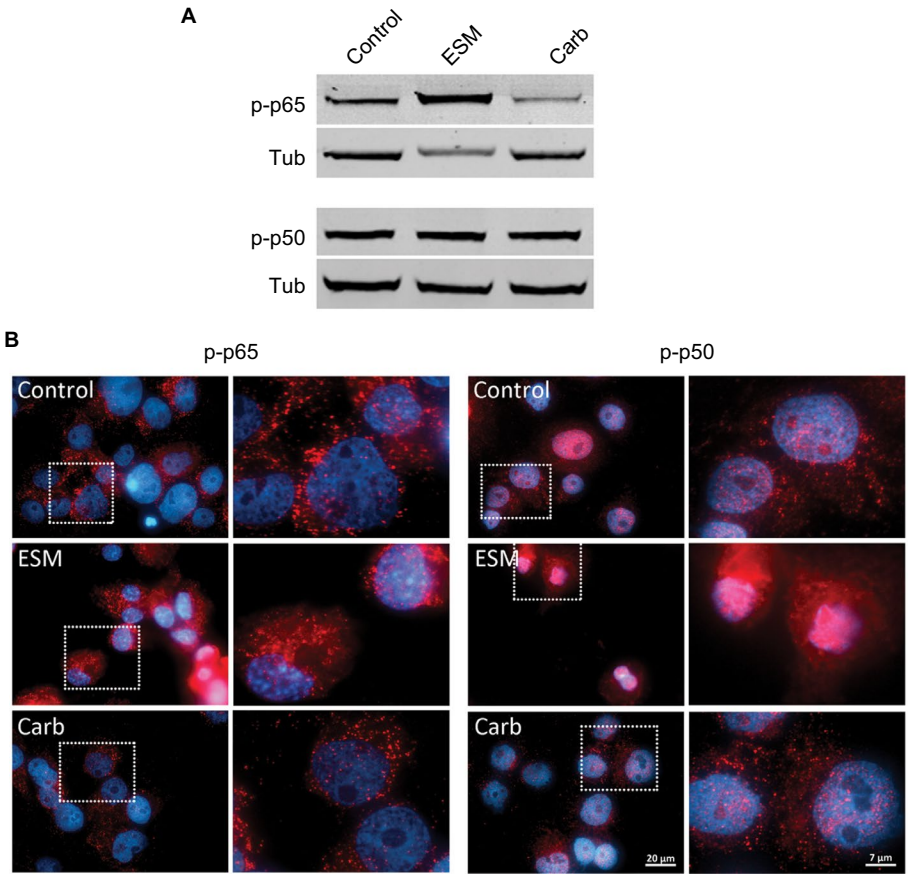

Figure 10 The activation of p65 and p50 subunits of NF-κB are differently regulated by ESM powder and carbohydrate fraction in macrophages.
Notes: PMA-differentiated THP-1 cells were incubated with 0.5 ng/mL LPS alone (control) or in combination with ESM (1 mg/mL) or carbohydrate fraction (0.125 mg/mL) for 20 h at 37°C. (**A**) The cells were harvested and lysed in RIPA buffer. Equal volumes of whole cell lysates were subjected to Western blotting with antibodies against phospho-p65 and phospho-p50. A representative blot out of four experiments is shown. Tubulin was used as a loading control. (**B**) Cells were fixed in 4% PFA and then subjected to fluorescent immunostaining with primary antibodies against phospho-p65 or phospho-p50, and Alexa-546 conjugated goat-anti rabbit secondary antibodies (red). The nuclei were counterstained with Hoechst (blue). The boxed areas are presented at higher magnification and showed at the right panels. Scale bars as indicated.
Abbreviations: Carb, carbohydrate; PMA, phorbol 12-myristate 13-acetate; ESM, eggshell membrane, LPS, lipopolysaccharide, NF-κB, nuclear factor kappa B; p-p50, phospho-p50; p-p65, phospho-p65; Tub, tubulin; PFA, paraformaldehyde; RIPA, radioimmunoprecipitation assay buffer.

TLR4 results in cytokine production, which play a dominant role in the inflammatory response. It has been shown that upregulation of TLR4 contributes to sensitization of monocytes to LPS stimuli, whereas down-regulation decreases the pro inflammatory response.[38,39] Interestingly, the protein expression of ICAM1 was not reduced by ESM powder. ICAM1 is shown to participate in a feedback loop, directly affecting its own gene expression. Whether this could explain the lack of correlation between mRNA and protein level in upon ESM treatment is not known. The exact mechanism of ICAM1 and its role during inflammation is still unknown.[40]

To our surprise, the ESM powder also showed pro inflammatory properties with a modest increase in IL-1β and IL-6 secretion, and increased phosphorylation of NF-κB p65 subunit in inflammatory THP-1 macrophages. This is in contrast to the anti-inflammatory effects described above (increased IL-10 secretion, reduced NF-κB activity, and reduced TLR4 and ICAM1 gene expression). The reason for these discrepancies are not fully understood. One explanation can be that ESM triggers a transdifferentiation of macrophages from pro inflammatory cells (M1 macrophages) to anti-inflammatory cells (M2 macrophages). Supporting our assumption, we observed an increased expression of HO-1 upon treatment with ESM, concomitant with the expression of IL-10, at the investigated time points (Figure 6). HO-1 is generally highly expressed in M2 macrophages and has been reported to be closely involved in macrophage polarization toward an M2 phenotype.[41–43] The activation of HO-1 has been shown to inhibit the LPS-induced NF-κB activity in monocytes.[44] Several lines of evidences also suggested a vice versa relation between the HO-1 expression and IL-10 signaling.[44,45] Macrophage differentiation into pro inflammatory or anti-inflammatory cells depends on cell intrinsic NF-κB pathway activation, as well as the local cytokine environment (for review).[46] In vitro, the response of macrophages exposed to LPS occurs largely via TLR4 triggering NF-κB (p65 and p50)

activation and translocation to the nucleus where it promotes pro inflammatory cytokines (M1 macrophages). Exposure to certain cytokines such as IL-4 and IL-13, however, results in anti-inflammatory M2 macrophages producing lower amount of pro inflammatory mediators, but higher levels of anti-inflammatory mediators such as IL-10.[47,48] ESM represents a complex composition of ECM proteins, and might produce a milieu, triggering M2 macrophages that increases IL-10 secretion. Macrophages are regulators of both inflammation and its resolution, and NF-κB plays a key role in the instruction of macrophage responses. In our study, ESM powder increased post-translational modification (phosphorylation) of NF-κB p65 subunits in inflammatory THP-1 macrophages (Figure 10A). In mammals, the NF-κB family consists of several proteins, including NF-κB1 (p50), NF-κB2 (p52), RelA (p65), c-Rel (Rel), and Rel B. They function as transcription factors, translocated from an inactive state in cytoplasm to active dimers regulating gene expression in the nucleus. The dimers combination and phosphorylation pattern on the subunits determine their durability and signaling outcomes. Generally accepted, the classical NF-κB heterodimer composed of p50 and p65 units is a transcriptional activator of pro inflammatory cytokine expressions. The slight significant increase in pro inflammatory cytokine expression of IL-1β and IL-6 obtained for ESM in our study could be in line with these studies.[49,50] The role of NF-κB in regulation of pro inflammatory cytokine secretion is well recognized, but it also plays important role during IL-10 biosynthesis. Our data show translocation of phosphorylated p50 to the nucleus with ESM, and this is in line with previous work demonstrating that NF-κB p50 activating is involved in the increased production of the anti-inflammatory cytokine IL-10.[51,52] It has also been shown that p50 homodimers differentially regulates pro- and anti-inflammatory cytokines in macrophages, and that the p50 subunit can be transcriptional activators of IL-10 expression. Others have suggested that NF-κB may play a role in regulating early steps in IL-10 production through interactions with distal enhancers at the IL-10 locus.[53]

The events occurring during inflammation are more than just a simplistic interplay between pro- and anti-inflammatory cytokines. In fact, timing, concentration, and order of cytokines secreted, types of immune cells, amount, and ambiguity are all factors contributing to the complexity. For example, in order to measure the presence of secreted cytokines in THP-1 cells, long incubation times (often hours) are often necessary. This may turn on other signaling pathways. TNF-α accumulation is regulated by the anti-inflammatory cytokine IL-10, and IL-10 has been shown to suppress TNF-α production upon prolonged stimulation.[54] The amount of a cytokine clearly controls its properties. IL-12 is pro inflammatory in low doses, whereas 100-fold higher amounts were associated with an anti-inflammatory process.[55] Kinetic studies of TNF-α showed a decline after 24 h of LPS stimulation, while IL-10 accumulation increased after 18 h.[54] Ambiguity of cytokines is also an important factor during inflammation. IL-6 is mostly regarded as a pro inflammatory cytokine, but it also has anti-inflammatory activities.[56] Stimulation of myelin-reactive T cells with TGF-β plus IL-6 completely abrogated pathogenic function, and these cells failed to upregulate the pro inflammatory chemokines crucial for central nervous system inflammation. In addition, these cells produced IL-10, which has potent anti-inflammatory activities.[57]

Our experiments show that the carbohydrate fraction of the ESM also displays immunomodulating properties, suggesting that the carbohydrate proportion of ESM is an important component of the ESM powder. Interestingly, the immunomodulatory effect of the carbohydrate fraction was different: the secretion of IL-10 is unchanged, and IL-6 and IL-1β is reduced. This is in contrast to the results we observed with ESM powder. One explanation can be of the different physical and chemical properties of the two fractions. While the ESM powder is insoluble and retains the native fibrillary structure consisting of both proteins and carbohydrates, the isolated and soluble carbohydrate fraction might be more available in such affecting receptors and signaling pathways differently compared to the ESM. The carbohydrate fraction of ESM contains HA as the major GAG (81%), as well as minor amount of CS. Both HA and CS possess anti-inflammatory properties as demonstrated by others.[58–60] HA plays dual role during wound healing, and this is related to the sizes of the molecule.[9,10] After injury, CS/dermatan sulfate becomes soluble and is a major component in wound fluid.[9] CS has been demonstrated to decrease NF-κB translocation and reduce the formation of pro inflammatory cytokines such as IL-1β and TNF-α.[59] We did also see a slight decrease, but not significant, in CD44 mRNA gene expression. CD44 is the predominant receptor for high molecular weight HA in reducing pro inflammatory cytokine production.[29] A sustained expression of CD44 on the cell surface would favor the anti-inflammatory signaling of our carbohydrate fraction. The amount of N-glycan in the isolated carbohydrate fraction with molecular weight >6,000 Da is unknown, but probably not dominating as their size has been estimated to be ~2,000 Da. However, these N-glycans present in ESM could also be relevant immune modulators, as these structures have the capacity to regulate inflammatory responses as shown by others.[20,21]

Conclusion

In this study, we have demonstrated that the processed ESM powder obtains fibrillary structures similarly to the native ESM and is capable of modulating immune responses in vitro. The isolated carbohydrates part of ESM also displays immunomodulatory properties, suggesting that the carbohydrate proportion of ESM is an important component of the ESM powder. In conclusion, ESM powder and its carbohydrates part possess anti-inflammatory properties that make this material a promising ingredient suitable for use in wound treatment.

Acknowledgments

The authors want to thank Prof Rune Blomhoff at Institute of Basic Medical Sciences, University of Oslo, Oslo, Norway, for providing U937–3xκB-LUC cell line. They also thank Vibeke Høst and Bård Mathiesen for the excellent work with light microscopy and preparing the samples used in HPLC analysis, respectively. Also thanks to Prof Maxwell Hincke, Prof Matthias Schnabelrauch, Dr Enda Kenny, Dr Tamer Ahmed and Dr Annika Wartenberg for the feedback and discussions.

This work was supported by grant from Research Council of Norway (NFR 235545).

Disclosure

The authors report no conflicts of interest in this work.

References

1. Reinke JM, Sorg H. Wound repair and regeneration. *Eur Surg Res*. 2012;49(1):35–43.
2. Guarderas F, Leavell Y, Sengupta T, Zhukova M, Megraw TL. Assessment of chicken-egg membrane as a dressing for wound healing. *Adv Skin Wound Care.* 2016;29(3):131–134.
3. Liu Z, Zhang F, Li L, Li G, He W, Linhardt RJ. Compositional analysis and structural elucidation of glycosaminoglycans in chicken eggs. *Glycoconj J.* 2014;31(8):593–602.
4. Wong M, Hendrix MJ, von der Mark K, Little C, Stern R. Collagen in the egg shell membranes of the hen. *Dev Biol.* 1984;104(1):28–36.
5. Hincke MT, Gautron J, Panheleux M, Garcia-Ruiz J, McKee MD, Nys Y. Identification and localization of lysozyme as a component of eggshell membranes and eggshell matrix. *Matrix Biol.* 2000;19(5):443–453.
6. Cordeiro CM, Hincke MT. Quantitative proteomics analysis of eggshell membrane proteins during chick embryonic development. *J Proteomics.* 2016;130:11–25.
7. Gautron J, Hincke MT, Panheleux M, Garcia-Ruiz JM, Boldicke T, Nys Y. Ovotransferrin is a matrix protein of the hen eggshell membranes and basal calcified layer. *Connect Tissue Res.* 2001;42(4):255–267.
8. Cordeiro CM, Esmaili H, Ansah G, Hincke MT. Ovocalyxin-36 is a pattern recognition protein in chicken eggshell membranes. *PLoS One.* 2013;8(12):e84112.
9. Taylor KR, Gallo RL. Glycosaminoglycans and their proteoglycans: host-associated molecular patterns for initiation and modulation of inflammation. *FASEB J.* 2006;20(1):9–22.
10. Neuman MG, Nanau RM, Oruna-Sanchez L, Coto G. Hyaluronic acid and wound healing. *J Pharm Pharm Sci*: a publication of the Canadian Society for Pharmaceutical Sciences, Societe canadienne des sciences pharmaceutiques. 2015;18(1):53–60.
11. del Fresno C, Otero K, Gomez-Garcia L, et al. Tumor cells deactivate human monocytes by up-regulating IL-1 receptor associated kinase-M expression via CD44 and TLR4. *J Immunol.* 2005;174(5):3032–3040.
12. Schaefer L, Iozzo RV. Biological functions of the small leucine-rich proteoglycans: from genetics to signal transduction. *J Biol Chem.* 2010;283(31):21305–21309.
13. Tracy LE, Minasian RA, Caterson EJ. Extracellular matrix and dermal fibroblast function in the healing wound. *Adv Wound Care (New Rochelle).* 2016;5(3):119–136.
14. Kodali VK, Gannon SA, Paramasivam S, Raje S, Polenova T, Thorpe C. A novel disulfide-rich protein motif from avian eggshell membranes. *PLoS One.* 2011;6(3):e18187.
15. Kobayashi Y, Rupa P, Kovacs-Nolan J, Turner PV, Matsui T, Mine Y. Oral administration of hen egg white ovotransferrin attenuates the development of colitis induced by dextran sodium sulfate in mice. *J Agric Food Chem.* 2015;63(5):1532–1539.
16. Benson KF, Ruff KJ, Jensen GS. Effects of natural eggshell membrane (NEM) on cytokine production in cultures of peripheral blood mononuclear cells: increased suppression of tumor necrosis factor-alpha levels after in vitro digestion. *J Med Food.* 2012;15(4):360–368.
17. Shi Y, Rupa P, Jiang B, Mine Y. Hydrolysate from eggshell membrane ameliorates intestinal inflammation in mice. *Int J Mol Sci.* 2014;15(12):22728–22742.
18. Yoo J, Park K, Yoo Y, Kim J, Yang H, Shin Y. Effects of egg shell membrane hydrolysates on anti-inflammatory, anti-wrinkle, anti-microbial activity and moisture-protection. *Korean J Food Sci Anim Resour.* 2014;34(1):26–32.
19. Ruff KJ, DeVore DP. Reduction of pro-inflammatory cytokines in rats following 7-day oral supplementation with a proprietary eggshell membrane-derived product. *Modern Res Inflammat.* 2014;3(1):19–25.
20. Jefferis R. A sugar switch for anti-inflammatory antibodies. *Nat Biotechnol.* 2006;24(10):1230–1231.
21. Scott DW, Vallejo MO, Patel RP. Heterogenic endothelial responses to inflammation: role for differential N-glycosylation and vascular bed of origin. *J Am Heart Assoc.* 2013;2(4):e000263.
22. Landen NX, Li D, Stahle M. Transition from inflammation to proliferation: a critical step during wound healing. *Cell Mol Life Sci.* 2016;73(20):3861–3885.
23. Kim YH, Choi KH, Park JW, Kwon TK. LY294002 inhibits LPS-induced NO production through a inhibition of NF-kappaB activation: independent mechanism of phosphatidylinositol 3-kinase. *Immunol Lett.* 2005;99(1):45–50.
24. Lu YC, Yeh WC, Ohashi PS. LPS/TLR4 signal transduction pathway. *Cytokine.* 2008;42(2):145–151.
25. Roebuck KA, Finnegan A. Regulation of intercellular adhesion molecule-1 (CD54) gene expression. *J Leukoc Biol.* 1999;66(6):876–888.
26. Paulsen K, Tauber S, Dumrese C, et al. Regulation of ICAM-1 in cells of the monocyte/macrophage system in microgravity. *Biomed Res Int.* 2015;2015:538786.
27. Schopohl P, Gruneberg P, Melzig MF. The influence of harpagoside and harpagide on TNFalpha-secretion and cell adhesion molecule mRNA-expression in IFNgamma/LPS-stimulated THP-1 cells. *Fitoterapia.* 2016;110:157–165.
28. Maytin EV. Hyaluronan: more than just a wrinkle filler. *Glycobiology.* 2016;26(6):553–559.
29. Nakamura K, Yokohama S, Yoneda M, et al. High, but not low, molecular weight hyaluronan prevents T-cell-mediated liver injury by reducing pro-inflammatory cytokines in mice. *J Gastroenterol.* 2004;39(4):346–354.
30. Grondahl F, Tveit H, Akslen-Hoel LK, Prydz K. Easy HPLC-based separation and quantitation of chondroitin sulphate and hyaluronan disaccharides after chondroitinase ABC treatment. *Carbohydr Res.* 2011;346(1):50–57.

31. Moen A, Hafte TT, Tveit H, Egge-Jacobsen W, Prydz K. N-Glycan synthesis in the apical and basolateral secretory pathway of epithelial MDCK cells and the influence of a glycosaminoglycan domain. *Glycobiology.* 2011;21(11):1416–1425.
32. Carlsen H, Moskaug JO, Fromm SH, Blomhoff R. In vivo imaging of NF-kappa B activity. *J Immunol.* 2002;168(3):1441–1446.
33. Balaz M. Eggshell membrane biomaterial as a platform for applications in materials science. *Acta Biomater.* 2014;10(9):3827–3843.
34. Sabat R, Grutz G, Warszawska K, et al. Biology of interleukin-10. *Cytokine Growth Factor Rev.* 2010;21(5):331–344.
35. Nomura F, Akashi S, Sakao Y, et al. Cutting edge: endotoxin tolerance in mouse peritoneal macrophages correlates with down-regulation of surface toll-like receptor 4 expression. *J Immunol.* 2000;164(7):3476–3479.
36. Zarember KA, Godowski PJ. Tissue expression of human Toll-like receptors and differential regulation of Toll-like receptor mRNAs in leukocytes in response to microbes, their products, and cytokines. *J Immunol.* 2002;168(2):554–561.
37. Medvedev AE, Kopydlowski KM, Vogel SN. Inhibition of lipopolysaccharide-induced signal transduction in endotoxin-tolerized mouse macrophages: dysregulation of cytokine, chemokine, and toll-like receptor 2 and 4 gene expression. *J Immunol.* 2000;164(11):5564–5574.
38. Abreu MT, Vora P, Faure E, Thomas LS, Arnold ET, Arditi M. Decreased expression of Toll-like receptor-4 and MD-2 correlates with intestinal epithelial cell protection against dysregulated proinflammatory gene expression in response to bacterial lipopolysaccharide. *J Immunol.* 2001;167(3):1609–1616.
39. Tamandl D, Bahrami M, Wessner B, et al. Modulation of toll-like receptor 4 expression on human monocytes by tumor necrosis factor and interleukin-6: tumor necrosis factor evokes lipopolysaccharide hyporesponsiveness, whereas interleukin-6 enhances lipopolysaccharide activity. *Shock.* 2003;20(3):224–229.
40. Hoesel B, Schmid JA. The complexity of NF-κB signaling in inflammation and cancer. *Mol Cancer.* 2013;12(1):86.
41. Weis N, Weigert A, von Knethen A, Brune B. Heme oxygenase-1 contributes to an alternative macrophage activation profile induced by apoptotic cell supernatants. *Mol Biol Cell.* 2009;20(5):1280–1288.
42. Montana G, Lampiasi N. Substance P induces HO-1 expression in RAW 264.7 cells promoting switch towards M2-Like macrophages. *PLoS One.* 2016;11(12):e0167420.
43. Dai M, Wu L, He Z, et al. Epoxyeicosatrienoic acids regulate macrophage polarization and prevent LPS-induced cardiac dysfunction. *J Cell Physiol.* 2015;230(9):2108–2119.
44. Drechsler Y, Dolganiuc A, Norkina O, et al. Heme oxygenase-1 mediates the anti-inflammatory effects of acute alcohol on IL-10 induction involving p38 MAPK activation in monocytes. *J Immunol.* 2006;177(4):2592–2600.
45. Sierra-Filardi E, Vega MA, Sánchez-Mateos P, Corbí AL, Puig-Kröger A. Heme Oxygenase-1 expression in M-CSF-polarized M2 macrophages contributes to LPS-induced IL-10 release. *Immunobiology.* 2010;215(9–10):788–795.
46. Hayden MS, Ghosh S. NF-κB in immunobiology. *Cell Research.* 2011;21(2):223–244.
47. Stein M, Keshav S, Harris N, Gordon S. Interleukin 4 potently enhances murine macrophage mannose receptor activity: a marker of alternative immunologic macrophage activation. *J Exp Med.* 1992;176(1):287–292.
48. Varin A, Gordon S. Alternative activation of macrophages: immune function and cellular biology. *Immunobiology.* 2009;214(7):630–641.
49. Barnes PJ, Karin M. Nuclear factor-kappaB: a pivotal transcription factor in chronic inflammatory diseases. *N Engl J Med.* 1997;336(15):1066–1071.
50. Karin M, Lin A. NF-kappaB at the crossroads of life and death. *Nat Immunol.* 2002;3(3):221–227.
51. Cao S, Zhang X, Edwards JP, Mosser DM. NF-kappaB1 (p50) homodimers differentially regulate pro- and anti-inflammatory cytokines in macrophages. *J Biol Chem.* 2006;281(36):26041–26050.
52. Driessler F, Venstrom K, Sabat R, Asadullah K, Schottelius AJ. Molecular mechanisms of interleukin-10-mediated inhibition of NF-κB activity: a role for p50. *Clin Exp Immunol.* 2004;135(1):64–73.
53. Saraiva M, Christensen JR, Tsytsykova AV, et al. Identification of a macrophage-specific chromatin signature in the IL-10 locus. *J Immunol.* 2005;175(2):1041–1046.
54. Chanput W, Mes J, Vreeburg RA, Savelkoul HF, Wichers HJ. Transcription profiles of LPS-stimulated THP-1 monocytes and macrophages: a tool to study inflammation modulating effects of food-derived compounds. *Food Funct.* 2010;1(3):254–261.
55. Kasama T, Yamazaki J, Hanaoka R, et al. Biphasic regulation of the development of murine type II collagen-induced arthritis by interleukin-12: possible involvement of endogenous interleukin-10 and tumor necrosis factor alpha. *Arthritis Rheum.* 1999;42(1):100–109.
56. Scheller J, Chalaris A, Schmidt-Arras D, Rose-John S. The pro- and anti-inflammatory properties of the cytokine interleukin-6. *Biochim Biophys Acta.* 2011;1813(5):878–888.
57. McGeachy MJ, Bak-Jensen KS, Chen Y, et al. TGF-beta and IL-6 drive the production of IL-17 and IL-10 by T cells and restrain T(H)-17 cell-mediated pathology. *Nat Immunol.* 2007;8(12):1390–1397.
58. Aya KL, Stern R. Hyaluronan in wound healing: rediscovering a major player. *Wound Repair Regen.* 2014;22(5):579–593.
59. du Souich P, Garcia AG, Verges J, Montell E. Immunomodulatory and anti-inflammatory effects of chondroitin sulphate. *J Cell Mol Med.* 2009;13(8A):1451–1463.
60. Campo GM, Avenoso A, Campo S, et al. Glycosaminoglycans modulate inflammation and apoptosis in LPS-treated chondrocytes. *J Cell Biochem.* 2009;106(1):83–92.